REPORT DOCUMENTATION PAGE

Form Approved
OMB No. 0704-0188

2. REPORT DATE	3. REPORT TYPE AND DATES COVERED
April 2, 1994	January 1, 1993 - April 23, 1994

4. TITLE AND SUBTITLE

NMR Relaxation Behavior of The Head Group of SHBS in Lamellar Liquid Crystals

5. FUNDING NUMBERS

PE-N0014-91
PR-1274

6. AUTHOR(S)

Joseph R. Duke and Frank D. Blum

7. PERFORMING ORGANIZATION NAME(S) AND ADDRESS(ES)

University of Missouri-Rolla
Department of Chemistry
Rolla, MO 65401
ATTN: Frank D. Blum

8. PERFORMING ORGANIZATION REPORT NUMBER

UMR-FDB- 38

9. SPONSORING/MONITORING AGENCY NAME(S) AND ADDRESS(ES)

Office of Naval Research - Code 5000
Chemistry Division
800 Quincy Street
Arlington, VA 22217
ATTN: Kenneth J. Wynne

10. SPONSORING/MONITORING AGENCY REPORT NUMBER

11. SUPPLEMENTARY NOTES

For publication in Langmuir

12a. DISTRIBUTION/AVAILABILITY STATEMENT

Unlimited - Approved for unlimited public release

12b. DISTRIBUTION CODE

13. ABSTRACT *(Maximum 200 words)*

Deuterium NMR relaxation-time constants T_{1Q} and T_{1Z}, from spectra of a phenyl-ring-deuterated double-tailed surfactant, sodium 4-(1'-heptylnonyl)benzenesulfonate (SHBS) in liquid crystals formed with water were obtained from 0 to 80 °C. The relaxation-time constants were determined for the 15 and 90 degree orientations of the powder sample. This data is compared to predicted relaxation time constants from two different models for molecular reorientation, including: (I) phenyl-rings undergoing uniaxial reorientation about the 1'-4' axis; (II) phenyl-rings rotating rapidly about the 1'-4' axis of a molecule which is reorienting about a space fixed director axis. Both models include an adjustable parameter that describes molecular motion about the 1'-4' axis that results from either strong collisions or small step free rotational diffusion. The results from both models indicate the rate of reorientation about the 1'-4' axis of the phenyl ring is approximately three times the nuclear Larmor frequency of the deuterium nucleus, 30 MHz, at room temperature. This rate increases with increasing temperature. The best fits of the data were determined using model (II). The predicted rate constants for motion about this axis differ slightly for each model, whereas, the type of motion predicted by the two models is very different. Model (I) indicates reorientation about the 1'-4' axis is more like strong collisions. Model (II) indicates that the motion is more like small step rotational diffusion.

14. SUBJECT TERMS

Surfactants, interfaces, dynamics, deuterium NMR

15. NUMBER OF PAGES

27

16. PRICE CODE

17. SECURITY CLASSIFICATION OF REPORT	18. SECURITY CLASSIFICATION OF THIS PAGE	19. SECURITY CLASSIFICATION OF ABSTRACT	20. LIMITATION OF ABSTRACT
Unclassified	Unclassified	Unclassified	

OFFICE OF NAVAL RESEARCH

Grant N00014-91-J-1274

R&T Code 413m005---04

Technical Report # UMR-FDB-38

NMR Relaxation Behavior of the Head Group in Lamellar Liquid Crystals

by

Joseph R. Duke and Frank D. Blum

Department of Chemistry and Materials Research Center
University of Missouri-Rolla
Rolla, MO 65401

(314) 341-4451

Prepared for Publication in

Langmuir

April 23, 1994

Abstract

Deuterium NMR relaxation-time constants T_{1Q} and T_{1Z}, from spectra of a phenyl-ring-deuterated double-tailed surfactant, sodium 4-(1'-heptylnonyl)benzenesulfonate (SHBS) in liquid crystals formed with water were obtained from 0 to 80 °C. The relaxation-time constants were determined for the 15 and 90 degree orientations of the powder sample. This data is compared to predicted relaxation time constants from two different models for molecular reorientation, including: (I) phenyl-rings undergoing uniaxial reorientation about the 1'-4' axis; (II) phenyl-rings rotating rapidly about the 1'-4' axis of a molecule which is reorienting about a space fixed director axis. Both models include an adjustable parameter that describes molecular motion about the 1'-4' axis that results from either strong collisions or small step free rotational diffusion. The results from both models indicate the rate of reorientation about the 1'-4' axis of the phenyl ring is approximately three times the nuclear Larmor frequency of the deuterium nucleus, 30 MHz, at room temperature. This rate increases with increasing temperature. The best fits of the data were determined using model (II). The predicted rate constants for motion about this axis differ slightly for each model, whereas, the type of motion predicted by the two models is very different. Model (I) indicates reorientation about the 1'-4' axis is more like strong collisions. Model (II) indicates that the motion is more like small step rotational diffusion.

Introduction

Surfactants in water can be molecularly dispersed like other solutes at low concentrations. With increasing concentration, the surfactant may micellize, or separate from the solution as an ordered phase. The separated phase may be either crystalline or liquid crystalline. The type of behavior observed depends upon many parameters, including the structure of the surfactant and the temperature of the system.

Lamellar or smectic liquid crystalline dispersions have been used in a variety of different applications. The applications include tertiary oil recovery (1), drug delivery (2), and model membranes (3). In lamellar liquid crystals, the surfactant forms bilayers which separate the water layers. These systems show both long range order and local translational and rotational mobility for various chemical moieties comprising the system.

Sodium 4-(1'-heptylnonyl)benzenesulfonate (SHBS) is a double-tailed surfactant that has properties similar to many molecules of synthetic or biological origin. The surfactant shows no critical micelle concentration in water, but does show some evidence of aggregation below its solubility limit. At higher surfactant concentrations, liquid crystals form and coexist with the soluble surfactant (4-6). Aqueous dispersions of these liquid crystals may be sonicated to form vesicles (7-10) and mechanically agitated to form liposome type structures (11). The liquid crystals of SHBS and water do not appear to orient in a magnetic field, at 4.7 T, and form polycrystalline samples. Consequently, the individual lamellar domains are randomly oriented, with respect to the magnetic field throughout the sample.

In order to investigate the motion of the headgroup, the phenyl protons of SHBS have been replaced with deuterons. The phenyl group is then the "labeled" site and used as a reporter group for the headgroup motions. The structure of the molecule is shown below.

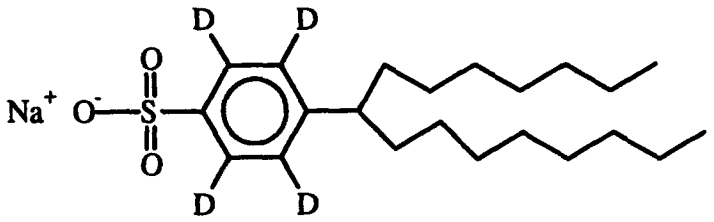

Sodium 4-(1'-heptylnonyl)benzenesulfonate

A previous study of SHBS liquid crystals compared experimental D-NMR lineshapes with lineshapes simulated for three different types of molecular reorientation (12). Simulated spectra for the case of a fast uniaxial reorientation about the molecule fixed 1'-4' axis have similar line shapes, but quadrupolar splittings are not reduced as much as those of the experimental spectra (12-14). For what is usually called *anisotropic rotational diffusion*, a fast motion about the 1'-4' molecular axis of the phenyl ring and a much slower motion perpendicular to this axis are considered. Simulated spectra based on this anisotropic rotational diffusion have quadrupolar splittings which are similar to the experimental ones, but the lineshapes are not reproduced well (12,15). The addition of what has been termed "*anisotropic viscosity*" (16) has been used to produce simulated spectra which have both quadrupolar splittings and lineshapes which match the experimental spectra. With anisotropic viscosity, the motion the deuterated phenyl ring is modeled as a fast reorientation of the molecule about a space fixed director axis (1'-4" axis) and a fast motion perpendicular to this axis that is restricted by an intermolecular interaction. Shown in Figure 1 are spectra calculated using the anisotropic rotational diffusion and anisotropic viscosity models along with an experimental spectrum.

Relaxation Behavior. In this paper, we have furthered our studies of the SHBS water system with relaxation measurements. Relaxation rates of deuterium nuclear magnetic resonance (D-NMR) spectra are often measured using inversion-recovery (IR) (17-19) and Jeener-Broekaert (JB) excitation experiments (20) in studies of molecular dynamics in liquid crystalline systems. Orientation dependent information is readily available from the inversion recovery experiment and

anisotropies in Zeeman relaxation rates R_{1Z} can be measured and used to compare various models of molecular reorientation (19). Orientation dependent information is also available from the JB pulse sequence, but this pulse sequence has been limited to use in macroscopically oriented systems. A broadband version of the JB pulse sequence (BBJB) has recently been developed for excitation of quadrupolar polarization over a wide frequency range. This has allowed powder samples to be studied with these techniques and orientation dependent quadrupolar relaxation rates R_{1Q} to be determined (21-23).

The IR and BBJB experiments can be used to measure both spectral densities $J_1(\omega_0)$ and $J_2(2\omega_0)$, from relaxation rate data for the recovery of Zeeman and quadrupolar polarization (19),

$$R_{1Z} = \frac{3\pi^2}{2}(e^2qQ/h)^2\,[J_1(\omega_0) + 4J_2(2\omega_0)] \qquad (1)$$

and,

$$R_{1Q} = \frac{9\pi^2}{2}(e^2qQ/h)^2\,J_1(\omega_0) \qquad (2)$$

where, (e^2qQ/h) is the quadrupolar coupling constant, in Hz, and the relaxation rates R_{1Z} and R_{1Q} are related to the relaxation time constants T_{1Z} and T_{1Q} with the following equation, $R_{1Z(Q)} = 1/T_{1Z(Q)}$. The spectral densities provide information on molecular motion as a function of frequency. The relaxation rates for different orientations of microcrystallites with respect to the magnetic field will, in general, be different and are used for comparison with the predicted relaxation rates from various models. For powdered samples, this involves measuring the relaxation rates for different portions of the spectrum corresponding to different orientations of the microcrystallites with respect to the magnetic field.

Motional Models The interpretation of the relaxation data, in this paper, is based on fitting it to two different, but related, motional models. Model (I) is based on uniaxial molecular reorientation for various orientations of the molecular diffusion axis with respect to the magnetic field (19,24,25). Model (II) is a composite model based on both an internal uniaxial segmental

reorientation and on an overall reorientation of the molecule with respect to a space fixed director axis. Both models use the same mathematical description for the uniaxial reorientation.

Uniaxial reorientation may involve a continuous small step diffusive type motion or strong collisions which cause the molecule to jump from one site to any other of the N sites equally spaced about the molecular diffusion axis. For molecules reorienting uniaxially in an oriented sample and in the fast motion limit, $\tau_c < 10^{-7}$ s, the lineshape is fully collapsed to what is expected for a motionally averaged quadrupolar tensor. With either jumps or continuous diffusion about the molecular diffusion axis the D-NMR spectrum would appear as a doublet. For a powdered sample, these two types of fast motions would yield characteristic powder patterns (12-14). When N is large the distinction between strong collisions and small step rotational diffusion is not obvious from line shape analysis alone. In this case, relaxation rate measurements may help to probe the mechanistic details of uniaxial molecular reorientation (19).

When the N sites that the molecule may occupy are equally spaced about the molecular diffusion axis, there are three possible types of motions that have been treated by Torchia and Szabo (24): nearest neighbor jumps; jumps from one site to any other (strong collisions); and free diffusion. As the number of sites approaches infinity, the solution for nearest neighbor jumps is equivalent to the solution for free diffusion. A solution for the correlation functions of motion about the molecular diffusion axis, $f_{LL'}(t)$, that incorporates both free diffusion and strong collision models is (26),

$$f_{L,L'}(\tau_L) = \delta_{L,L'}\, e^{-t/\tau_L} \qquad (3)$$

where, the two significant correlation times τ_1 and τ_2 are related by the equation $\tau_1 = (3p + 1)\tau_2$, $\delta_{LL'}$ is the delta function for states L and L', and p describes the type of motion. When the variable p = 1, the solution corresponds to small step rotational diffusion and when p = 0 the solution corresponds to strong collisions. Intermediate values of p correspond to a mixture of the two types of reorientation. This solution is applicable to both models (I) and (II). It describes the

uniaxial motion about the molecular diffusion axis in model (I) and the internal uniaxial segmental motion of model (II).

In addition to the uniaxial segmental reorientation, model (II) incorporates a description of an overall reorientation of the entire molecule about a space fixed director axis to calculate relaxation time constants (26). In this model, there are four parameters that describe molecular reorientation. They describe the rate of uniaxial segmental reorientation, the type of segmental motion, (small step diffusion or strong collisions), and two rates of molecular reorientation with respect to the director axis (one rate describes the reorientation of the molecule away from the director axis, and the other describes rotation of the molecule about this axis). The motions of the molecule about and away from the director axis are influenced by a restoring potential which mimics intermolecular interactions. The spectral densities, in equation 1 and 2, can be calculated, for a given angle between the director axis and the static magnetic field, from a table of numerical values in the form of polynomials in the order parameter S_{ZZ} (26). The order parameter can be related to the residual quadrupolar splitting of the D-NMR spectrum and to the restoring potential (27).

Experimental

The deuteration of SHBS and preparation of liquid crystals were described previously (12). The liquid crystalline sample was formed from deuterium depleted water and surfactant. The overall composition of the liquid crystalline sample is 40 wt % water 60 wt % SHBS. The sample was allowed to equilibrate at room temperature, then it was placed in the probe, brought to the desired temperature, and allowed to stay at that temperature until echo spectra showed no further changes in quadrupolar splitting. Then, relaxation experiments were performed. The temperatures at which relaxation rates were determined ranged from 0° to 80° C.

The deuterium relaxation experiments were performed with a Varian VXR-200 spectrometer operating with a wide line probe at 30.7 MHz for deuterium. The T_{1Z}'s were determined using the inversion-recovery pulse sequence with a quadrupolar echo for acquisition to avoid receiver deadtime.

$$(\pi) - t - (\pi/2)_x - \tau - (\pi/2)_y - \tau - \text{acquire}$$

A set of spectra were recorded at each temperature using this pulse sequence. The time, t, between the π pulse and the quadrupolar-echo pulse pair was arrayed in this set of spectra to obtain the time constant T_{1z}. The pulse widths were set at 2.0 μs for the $\pi/2$ pulse. The delay used in the quadrupolar echo pulse pair, τ, was set to 40 μs. A total of 4096 data points, both real and imaginary, were recorded with a spectral width of 150 kHz for each transient.

In order to measure T_{1Q} in powder samples, like SHBS liquid crystals, excitation over a wide range of frequencies is necessary. Broadband excitation pulse sequences allow this type of excitation. We have used a BBJB excitation pulse sequence, developed by Wimperis and Bodenhausen (21,22), and combined it with a $\pi/2$ refocusing pulse in the detection period (28) to create quadrupolar polarization and to measure T_{1Q}. The pulse sequence and phase cycling employed avoid problems related to phase corrections and frequency discrimination of other JB pulse sequences and allow only the recovery of quadrupolar polarization to be monitored.

$$(\pi/2)\text{-}\ \tau\ \text{-}\ (2\pi/6)\ \text{-}\ 2\tau\ \text{-}\ (\pi/12)\ \text{-}\ t\ \text{-}\ \ (\pi/4)\ \text{-}\ \tau'\ \text{-}\ (\pi/2)\text{-}\ \tau'\ \text{-acquire}$$

A set of spectra were recorded at each temperature using this pulse sequence. The first three pulses create the quadrupolar excitation. The last two pulses are used to monitor the remaining signal. In this set of experiments the time, t, between the third an fourth pulses was arrayed to obtain the time constant T_{1q}. The π pulse width was adjusted to 2.4 microseconds. The time τ used in the quadrupolar excitation portion of the pulse sequence was determined (17) using the average of the frequencies of the 15° and 90° orientations, at each temperature. The time τ' used in the monitoring portion of the sequence was set to 20 μs. A total of 4096 data points, both real and imaginary, were recorded with a spectral window size of 150 kHz for each transient.

The intensities were measured at the frequencies corresponding to the director of the microcrystallites being oriented at 90° and 15° with respect to the magnetic field. These positions are shown in Figure 1. The 90° orientation was chosen because of its intensity, however, intensity from the 35.7 degree orientation also contributes to the intensity at this frequency. The 15° orientation was chosen because there is a significant amount of intensity, and no spectral overlap at this point in the spectrum. The relaxation time constants were then calculated from Equations 4 and 5 with a program that fits the data for I_0, I_∞ and $R_{(Z,Q)}$, using the Levenberg-Marquardt method (29).

$$I(t) = I_0 + (I_\infty - I_0)\ (1 - e^{-tR_{1Z}}) \tag{4}$$

and,

$$I(t) = I_0\ e^{-tR_{1Q}} \tag{5}$$

The relaxation rates determined from the time-intensity data were compared to relaxation rates generated using models (I) and (II). The χ^2 value of the following function was used to evaluate the best fit, which is the sum of four squared differences between the experimental (exp) and calculated (calc) values for the time constants at each of two orientations and relaxation times.

$$\chi^2 = \sum_{i=Z,\,Q} \sum_{j=15°,\,90°} \{T_{1i}^{exp}(j) - T_{1i}^{calc}(j)\}^2. \tag{6}$$

Results

The relaxation time constants from the inversion recovery and the broadband Jeener-Broekaert pulse experiments are listed in Table I. Under the BBJB pulse sequence, the measurement of the relaxation rate at 0 °C and the 15° orientation was not possible. The intensity corresponding to this orientation decayed very quickly, the signal to noise ratio at times greater than 20 μs was very poor, and the lineshape was distorted. Figures 2 and 3 show the Zeeman relaxation data for the 90 and 15° orientations of microcrystallites with respect to the magnetic field with temperature along with the fits from the two models (I and II) tested. Figures 4 and 5 show the corresponding data for the quadrupolar polarization relaxation times.

The experimental relaxation time constants were used, along with a quadrupolar coupling constant of 172 kHz (12), to determine the best p's and k's ($k=1/\tau$), given by Equation 3 for the uniaxial model (I), based on a minimum value of χ^2 from Equation 6. A diffusion angle of 60 degrees was used in the calculations, which is the angle between the diffusion axis and the C-D bond vector. The parameter p was varied from 0 to 1 in steps of 0.01, and k_1 was varied from 0.1 to 100 times the nuclear Larmor frequency (30.7 MHz). Table II lists the p's and k_1's that produce the best fits for each temperature studied using the uniaxial model.

In order to determine the effects that an overall molecular reorientation, about the liquid crystalline director axis, accompanied by phenyl ring rotation, about the 1'-4' axis, would have upon nuclear relaxation, spectral densities from the composite model (II) were used to generate relaxation data. A program called JC was used to generate the spectral densities (26). Relevant input parameters are the angle β (60 degrees), the form of the restoring potential (cosine), p--the type of reorientation, k_α, k_β, and k_γ, rotational rate constants and the order parameter S_{zz}. The order parameter was calculated from the experimentally determined quadrupolar splitting of the D-NMR spectrum at each temperature. S_{zz} can be related to the experimentally determined quadrupolar splitting of the D-NMR spectra at the 90 degree orientation, $\Delta\nu_q$, the frequency difference between the most intense parts of the D-NMR spectrum, using the following

relationship (12,27):

$$\Delta\nu_q = \frac{3}{2}\omega_q\left(\frac{3\cos^2\beta - 1}{2}\right)\left(\frac{3\cos^2\beta' - 1}{2}\right)S_{ZZ} \qquad (7)$$

where, the angle between the magnetic field and director, $\beta = 90°$, the angle between the C-D bond vector and the molecular diffusion axis, $\beta' = 60°$ and ω_Q is the quadrupolar coupling constant (12). The parameter p is the same as in model (I) and was varied from 0 to 1. The rate constant for phenyl ring rotation, k_γ or k_1 from model (I), was varied from 0.1 to 100 times the nuclear Larmor frequency. Its magnitude was at least 5 times k_α and k_β, the rate constants for molecular reorientation about the director axis. Further, k_α was set equal to k_β.

Reasonably good fits for all data sets were found when p was near 0.65. Decreasing k_α and k_β from 0.2 times k_γ increased the errors between calculated and experimental time constants. Table II shows the best k_γ's derived from the experimental quadrupolar splittings, using p = 0.65, and $k_\alpha = k_\beta = 5k_\gamma$. The table also shows the χ^2 values generated using both models (I) and (II).

Discussion

The use of the deuterium quadrupolar relaxation times to elucidate the dynamics of colloidal systems is not new. Spectral densities and reorientation times for water on cellulose, lamellar lyotropic liquid crystals, and nematic liquid crystals have all been measured. (30-33) These systems were oriented and only limited reports on unoriented samples have appeared. (34) For our powdered sample, the deuterium NMR lineshape consisted of superpositions of the two transitions between nuclear spin states -1, 0, and 1, for molecules in microcrystallites at all orientations with respect to the magnetic field. The frequency that corresponds to the (-1 -> 0) transition for a molecule in a microcrystallite oriented at 90 degrees with respect to the magnetic field, is also the frequency that corresponds to the (0 -> 1) transition for a molecule in a microcrystallite oriented at 35.7 degrees with respect to the magnetic field, and vice versa. Thus, there will be contributions to the measured intensity, from both transitions, at this frequency. The relaxation rates for these two orientations may differ, resulting in a biexponential recovery of magnetization. The relative weights given to the two transitions in the biexponential recovery will be determined by several factors (19). This introduces from about a 3% to a 12% contribution from the 35.7 degree orientation to R_{1Z} measured at frequency corresponding to the 90 degree orientation of the microcrystallite (19). We have not included this factor in our calculations.

The inclusion of overall molecular reorientation (composite model) to the uniaxial motion reduces the error between the predicted and experimental relaxation times as seen in Figures 2 - 5 (also in the χ^2 values of Table II). The errors in measuring the relaxation rates caused by the overlapping of the two resonances may account for the small differences between the experimental data and the composite model, but not for the much larger differences between the experimental data and the uniaxial model.

The predicted rates for motion about the 1' - 4' axis differ only slightly between the two models over the entire temperature range studied. The reorientation rates predicted by the composite model are approximately 76% of those predicted by the uniaxial model. Both models

suggest the rate of reorientation is greater than three times the nuclear Larmor frequency at 0 °C and that this rate increases with temperature. The type of reorientation predicted for the two models differs significantly over the temperature range from 20 to 80 °C. The uniaxial model suggests this motion is more like a strong collision, $p \approx 0.3$. The type of motion suggested by the composite model is more like small step rotational diffusion, $p \approx 0.65$.

Activation energies for the rotation of the phenyl ring about the 1'-4' axis can be determined from plots of ln(1/k) vs. 1/T (25). Figure 6 is a graphical representation of the predicted correlation times log 1/k with 1/T. The data points used to plot log(1/k) vs. 1/T are not linear as can be seen from a best fit line through the predicted points. We have, however, used the slope of the line to determine the apparent activation energy for rotation of the phenyl ring about the 1'-4' axis. The deviation of the points from linearity may be a result of the varying composition of the liquid crystals with temperature. The system consisting of SHBS and water is known to be biphasic at 40% water and over the temperature range studied here. In the biphasic system, lamellar liquid crystals are known to be in equilibrium with a solution of solubilized surfactant. The liquid crystals contain approximately 25% water at room temperature, whereas the concentration of SHBS in water, at this temperature is less than 0.06%. At 90 °C the concentration of solubilized SHBS increases only to about 0.5%, while the liquid crystals may incorporate more water. For the case of the uniaxial model, the apparent activation energy is found to be 3.4 kcal/mole, for the composite model it is found to be 3.5 kcal/mole. These activation energies seem reasonable, they are approximately half of that determined for the phenyl ring of *p*-diethynylbenzene (DEB) dissolved in a nematic phase from Merck Licristal Phase 5 (26,32). The phenyl ring in our lyotropic phase appears to be less restricted to rotation than the DEB phenyl ring in the nematic phase. This is quite possible as the ionic repulsion between the headgroups and the double-tailed nature of the chains may give the headgroup more space to rotate than in the nematic phases.

In studies which have a site that can be labeled on the molecular diffusion axis the rate of molecular diffusion k_β can be determined (26,32). The structure of SHBS does not allow this information to be obtained. The use of k_γ at only 5 times the magnitude of k_α and k_β may be in

error, since the motion about the molecular diffusion axis should be much greater than the motion of the molecule about the director axis, for molecular motion about the axis to be uncoupled from the rotation of this axis. However, the fits to the data indicate that the inclusion of the composite motion can account for the relaxation times, in spite of this possible limitation.

Conclusions

Both models for molecular reorientation indicate that the motion of the phenyl ring is fast relative to the nuclear Larmor frequency between 20 and 80 °C. Both models predict similar rate constants for reorientation about the 1'-4' axis, but the type of motion predicted differs significantly. The composite model, incorporating phenyl ring rotation and anisotropic viscosity, fits the relaxation data better than the simpler uniaxial model. This is in agreement with an earlier lineshape study, which demonstrated that anisotropic viscosity could account for spectral lineshape. As shown previously, the internal rotation superimposed on the overall molecular reorientation in the presence of a restoring potential is necessary to account for the relaxation data in locally ordered systems (26). The relaxation rate data enabled the rates of motion of the phenyl ring to be quantified, whereas, lineshapes analysis was only effective in giving a type of molecular reorientation and a minimum rate for molecular reorientation. Together, the two studies provide complementary information on phenyl group reorientation in the smectic phase.

The excess water present in the sample containing liquid crystals of SHBS allows the liquid crystalline phase to incorporate more water at higher temperatures. The incorporation of excess water into the liquid crystals at higher temperatures was seen in a study of the binary system of SHBS and D_2O (35). The incorporation of water will affect the hydration of the sulfonate group and probably affect phenyl ring reorientation over this temperature range. This may be the reason for the deviation from linearity, of the Arrhennius plots, although the apparent energies of activation seem reasonable for this process.

Acknowledgments

The authors wish to thank Dr. Regitze Vold, of the University of California, San Diego, for the program used to calculate spectral densities for the composite model as well as other helpful information, Dr. Kenneth Jeffrey, of the University of Guelph, for information on the use of an echo pulse to follow the BBJB pulse sequence, and Dr. Steven Wimperis, of the University Chemical Laboratory, for the phase cycling used in the modified BBJB pulse sequence. We also acknowledge the Office of Naval Research for their financial support of the project.

References

1. Puig, J. E.; Frances, E. I.; Talmon, Y.; Davis, H. T.; Miller, W. G.; Scriven, L. E. *Soc. Pet. Eng. J.* **1982**, *22*, 37.
2. Szoka, F.; Padahadjopoulos, D *Ann. Rev. Bioeng.* **1980**, *9*,467.
3. Lee, A. G. *Prog. Biophys. Mol. Biol.* **1975**, *29*, 3.
4. Miller, W. G.; Blum, F. D.; Davis, H. T.; Franses, E. I.; Kaler, E. W.; Kilpatrick, P. K.; Nietering, K. E.; Puig, J. E.; Scriven, L. E.; In *Surfactants in Solution*, Vol. 1; Mittal, K. L., Lindman, B., Eds.; Plenum Publishing: New York, 1984, pp. 175.
5. Franses, E. I.; Davis, H. T.; Miller, W. G.; Scriven, L. E. *Chemistry of Oil Recovery*; Johansen, R. T., Berg, R. L., Eds.; American Chemical Society, Washington, D.C., 1979, pp. 35.
6. Kilpatrick, P. K.; Miller, W. G. *J. Phys. Chem.* **1984**, *88*, 1649.
7. Kilpatrick, P. K.; Miller, W. G.; Talmon, Y. *J. Colloid Interface Sci.* **1985**, *107*, 146.
8. Franses, E. I.; Talmon, Y.; Scriven, L. E.; Davis, H. T.; Miller, W. G. *J. Colloid Interface Sci.* **1982**, *86*, 449.
9. Kaler, E. W.; Falls, A. H.; Davis, T. H.; Scriven, L. E.; Miller, W. G. *J. Colloid Interface Sci.* **1982**, *90*, 424.
10. Madani, H.; Kaler, E. W. *Langmuir* **1990**, *6*, 125.
11. Blum, F. D.; Franses, E. I.; Rose, K. D.; Bryant, R. G.; Miller, W. G. *Langmuir* **1987**, *3*, 448.
12. Duke, J. R.; Funchess, B. F.; Blum, F. D. *Langmuir* **1991**, *7*, 1909.
13. Schmidt, C.; Wefing, S.; Blumich, B.; Speiss, H. W. *Chem. Phys. Lett.* **1986**, *130*, 84.
14. Cholli, A. L.; Dumais J. J.; Engle A. K.; Jelinski, L. W. *Macromolecules* **1984**, *17*, 2399.
15. Huntress, Jr., W. T. *Adv. Magn. Reson.* **1970**, *4*, 1.
16. Polnaszek, C. F.; Bruno, G. V.; Freed, J. H. *J. Chem. Phys.* **1973**, *58*, 3185.

17. Vold, R. L.; Dickerson, W. H.; Vold, R. R. *J. Magn. Reson.* **1981**, *43*, 213.

18. Ahmad, S. B.; Packer, K.J. *Molec. Phys.* **1979**, *37*, 47; and **1979**, *37*, 59.

19. Vold, R. R.; Vold R. L.; *Advances in Magnetic Resonance*, Vol. 16; Academic Press, Inc.: New York, 1991.

20. Jeener, J.; Broekaert, P. *Phys. Rev.* **1967**, *157*, 232.

21. Wimperis, S.; Bodenhausen, G. *Chem. Phys. Lett.* **1986**, *132*, 194.

22. Wimperis, S. *J. Magn. R eson.* **1990**, *86*, 46.

23. Hoatson, G. L.; Vold, R. L. *J. Magn. R eson.* **1992**, *98*, 342.

24. Torchia, D. A.; Szabo, A. *J. Magn. Reson.* **1982**, *49*, 107.

25. Wittebort, R. J.; Szabo, A. *J. Chem. Phys.* **1978**, *69*, 1722.

26. Vold, R. L.; Vold, R. R. *J. Chem. Phys.* **1988**, *88*, 1443.

27. Dong, R. Y. *Mol. Cryst. Liq. Cryst.* **1986**, *141*, 349.

28. Jeffrey, K. R. *Bull. Magn. Reson.* **1981**, *3*, 69.

29. *Numerical Recipes in C*, Press, W. H.; Flannery, B. P.; Teukolsky, S. A.; Vetterling, W. T., Eds.; Cambridge University Press: Cambridge, 1990.

30. Wong, T.C.; Ang, T.T. *J. Phys. Chem.*, **1985**, *89*, 4047.

31. Wong, T. C.; Jeffrey, K. R. *Mol. Phys.*, **1982**, *46*,1.

32. Dickerson, W. H.; Vold, R. R.; Vold, R. L.; *J. Phys. Chem.* **1983**, *87*, 166.

33. Dong, R. Y.; Richards, G.M. *Mol. Cryst. Liq. Cryst.* **1986**, *141*, 335.

34. Trouard, T.P.; Alam, T.M.; Zajicek, J.; Brown, M.F. *Chem. Phys. Lett.*, **1992**, *189*, 67.

35. Duke, J. R.; Blum, F. D.; unpublished results.

Table I

Relaxation time data (in ms) from the inversion-recovery and broadband Jeener-Broekaert experiments for the deuterons located on the phenyl ring of SHBS in the liquid crystalline phase oriented at 15° and 90° relative to the magnetic field axis. The uncertainties in the time constants based on the square roots of the relevant elements of the covariance matrices, are less than 3% of the values shown.

T (°C)	$T_{1Z}(90°)$	$T_{1Z}(15°)$	$T_{1Q}(90°)$	$T_{1Q}(15°)$
0	2.78	3.33	3.11	----
20	2.60	2.80	2.57	2.68
40	3.32	3.23	3.02	3.15
60	4.10	4.52	4.47	4.51
80	6.53	6.65	6.93	7.15

Table II

Best fit parameters for rotation of the phenyl ring of SHBS in the liquid crystalline phase using models (I) and (II). The parameters p and k_1 correspond to the uniaxial model (I) and the p' and k_γ correspond to the composite model.

	Model I			Model II		
T (°C)	p	k_1 (10^8 s^{-1})	χ^2	p'	k_γ (10^8 s^{-1})	χ^2
0	----	----	----	----	----	----
20	0.32	1.2	0.35	0.65	0.93	0.03
40	0.25	1.5	0.67	0.65	1.1	0.04
60	0.28	2.1	0.73	0.65	1.6	0.14
80	0.23	3.3	1.87	0.65	2.6	0.07

Figure Captions

Figure 1. Spectra calculated from the models of anisotropic rotational diffusion and anisotropic viscosity shown along with the experimental spectrum at 25° C (after reference 18). The frequencies corresponding to microcrystallites oriented at 15 and 90 degrees with respect to the magnetic field are shown on the experimental spectrum.

Figure 2. Inversion recovery relaxation time constants for microcrystallites located at 90 degrees with respect to the magnetic field for deuterons on the phenyl ring of SHBS in the liquid crystalline phase with temperature.

Figure 3. Inversion recovery relaxation time constants for microcrystallites located at 15 degrees with respect to the magnetic field for deuterons on the phenyl ring of SHBS in the liquid crystalline phase with temperature.

Figure 4. Broadband Jeener-Broekaert relaxation time constants for microcrystallites oriented at 90 degrees with respect to the magnetic field for deuterons on the phenyl ring of SHBS in the liquid crystalline phase with temperature.

Figure 5. Broadband Jeener-Broekaert relaxation time constants for microcrystallites oriented at 15 degrees with respect to the magnetic field for deuterons on the phenyl ring of SHBS in the liquid crystalline phase with temperature.

Figure 6. Predicted rate constants for phenyl ring reorientation about the 1'-4' axis for the uniaxial(●) and composite (▲) models as a function of temperature.

Figure 1

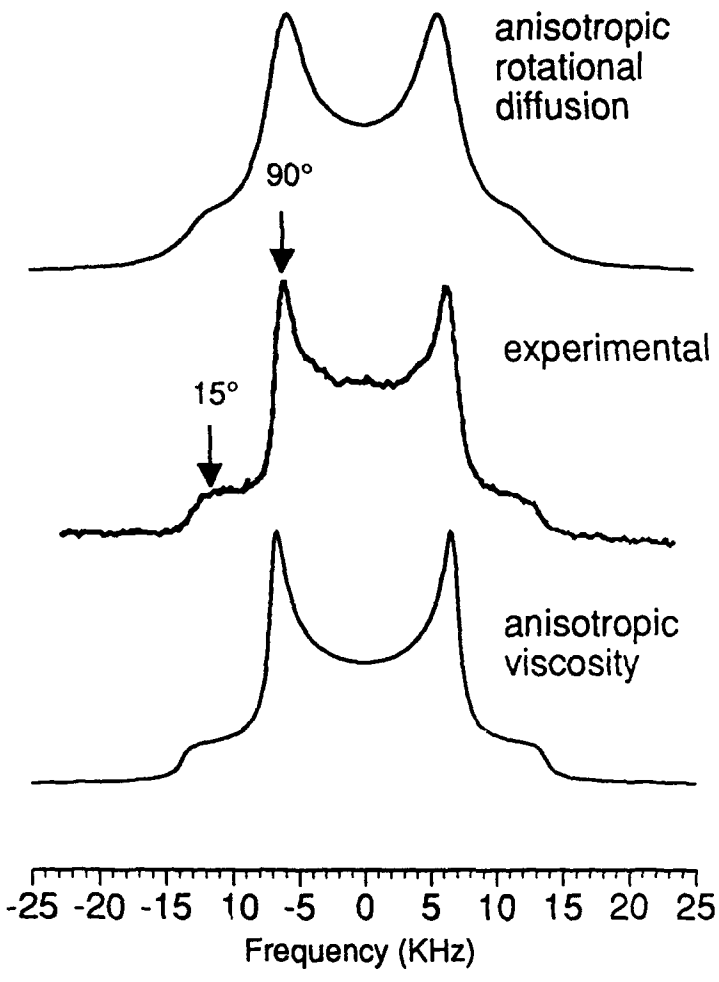

Figure 1. Spectra calculated from the models of anisotropic rotational diffusion and anisotropic viscosity shown along with the experimental spectrum at 25° C (after reference 18). The frequencies corresponding to microcrystallites oriented at 15 and 90 degrees with respect to the magnetic field are shown on the experimental spectrum.

Figure 2

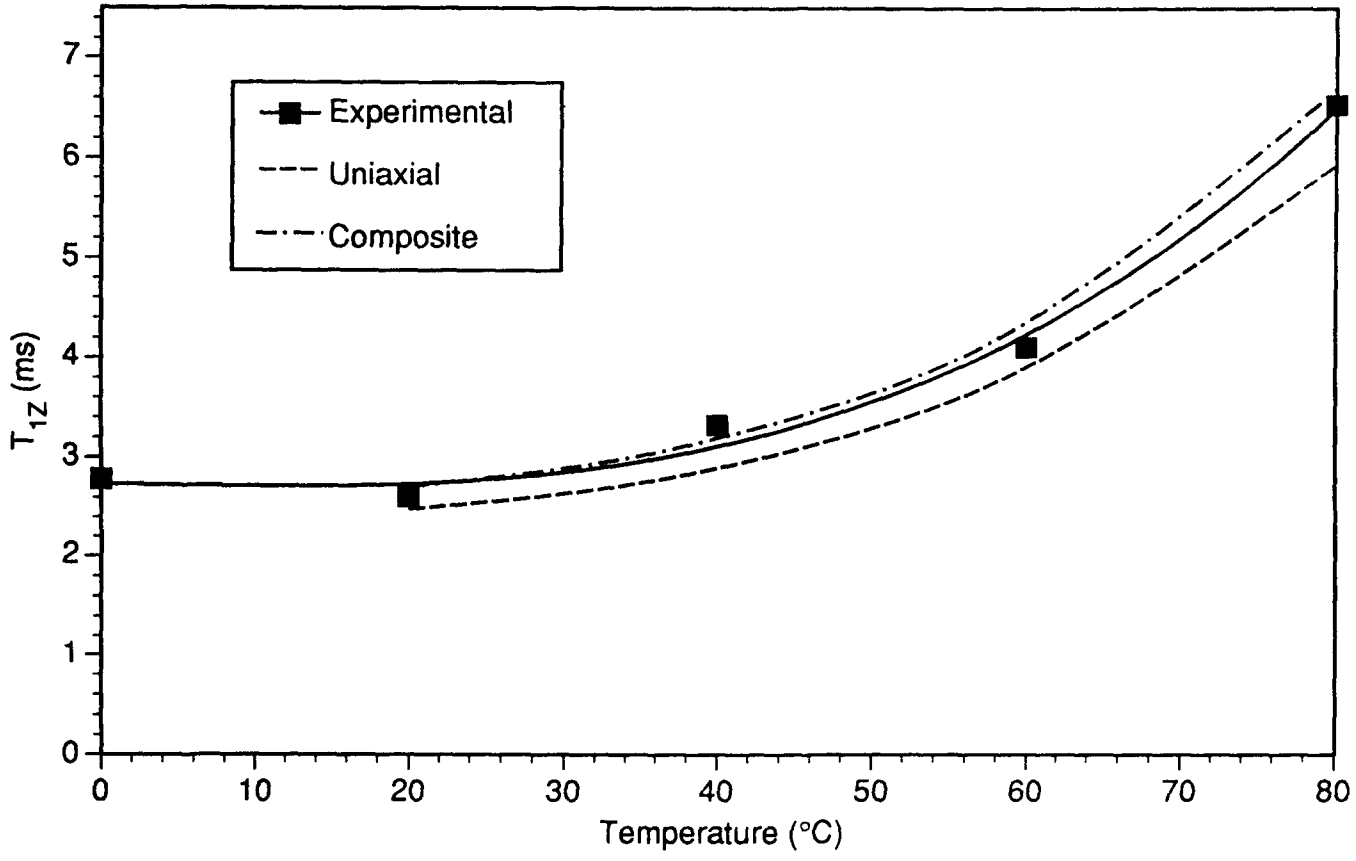

Figure 2. Inversion recovery relaxation time constants for microcrystallites located at 90 degrees with respect to the magnetic field for deuterons on the phenyl ring of SHBS in the liquid crystalline phase with temperature.

Figure 3

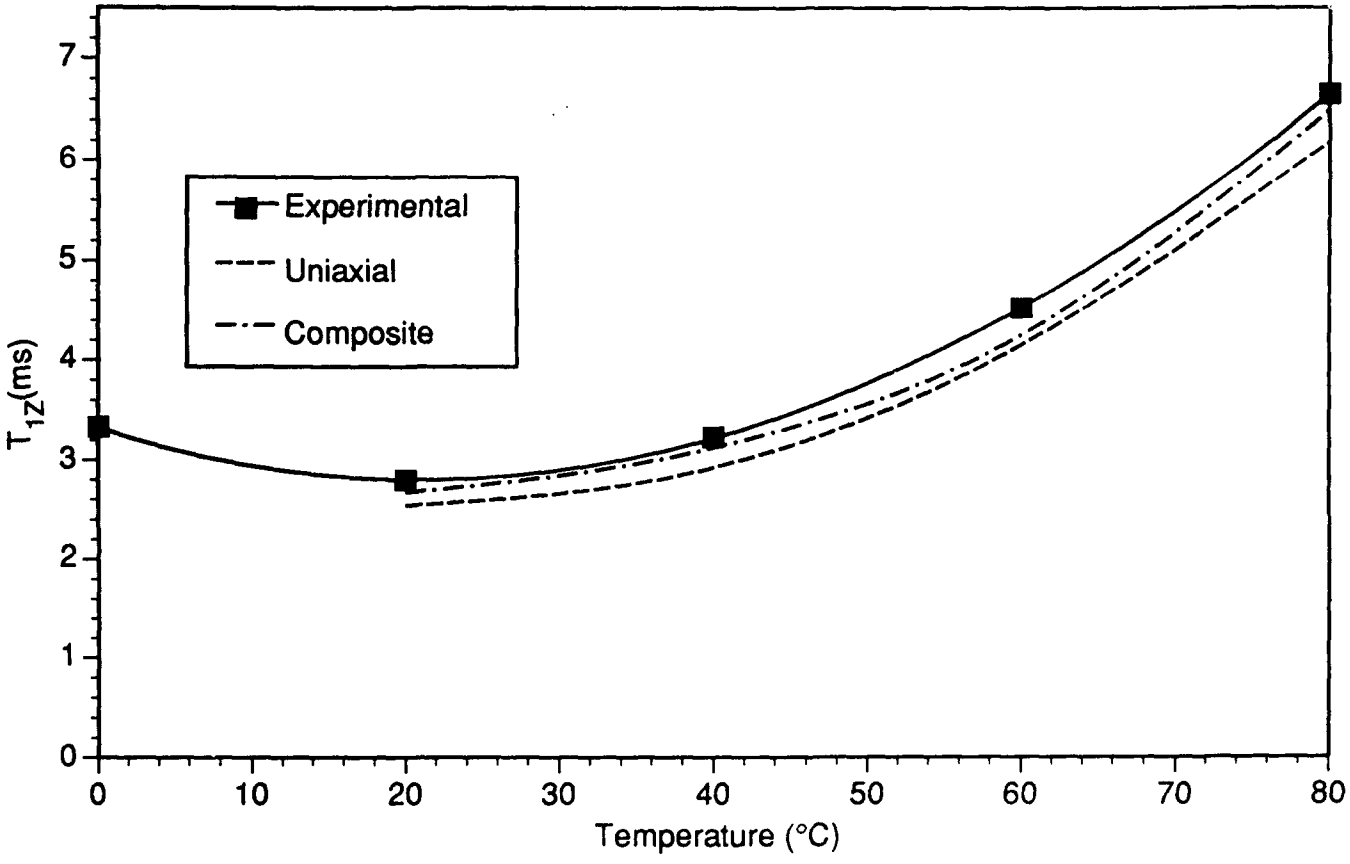

Figure 3. Inversion recovery relaxation time constants for microcrystallites located at 15 degrees with respect to the magnetic field for deuterons on the phenyl ring of SHBS in the liquid crystalline phase with temperature.

Figure 4

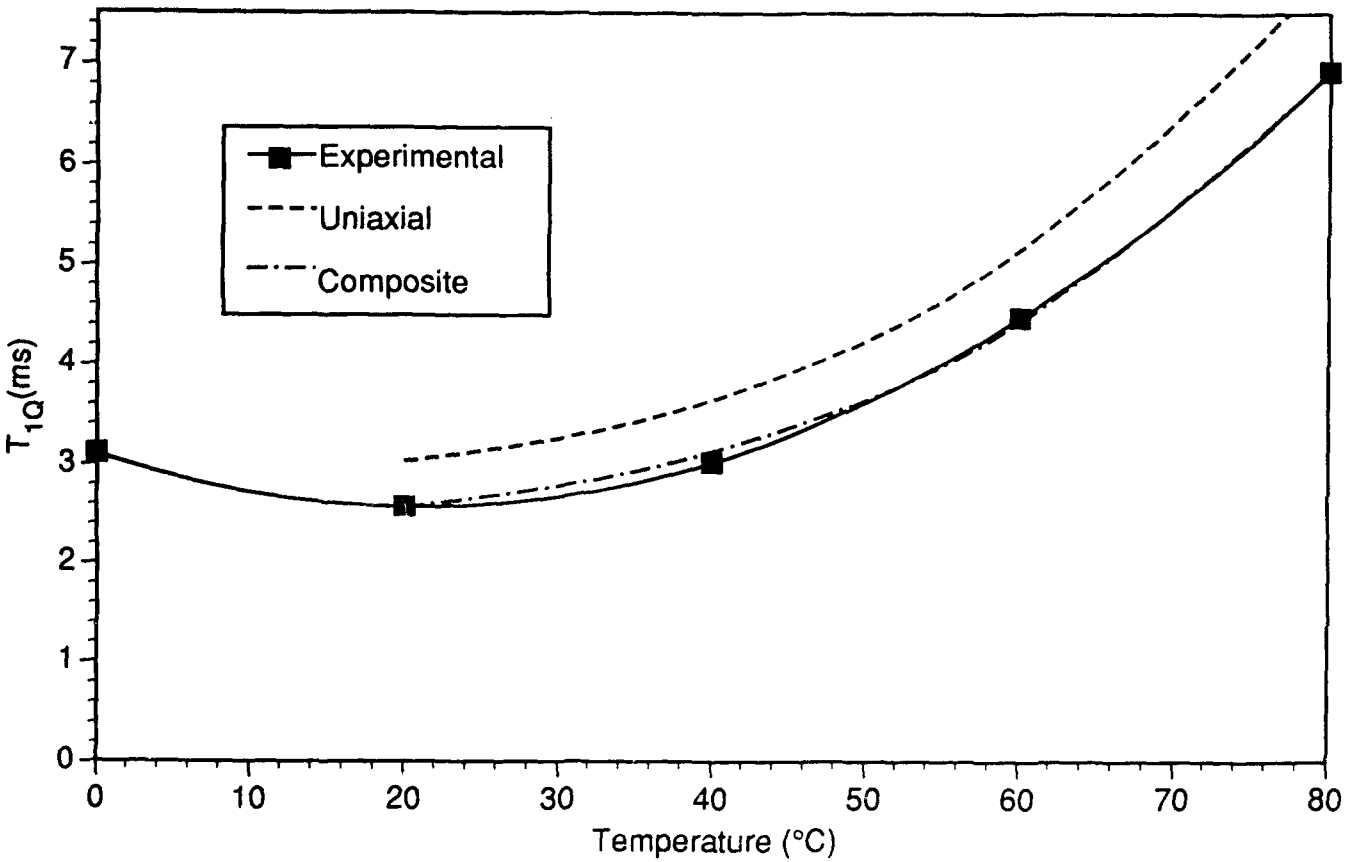

Figure 4. Broadband Jeener-Broekaert relaxation time constants for microcrystallites oriented at 90 degrees with respect to the magnetic field for deuterons on the phenyl ring of SHBS in the liquid crystalline phase with temperature.

Figure 5

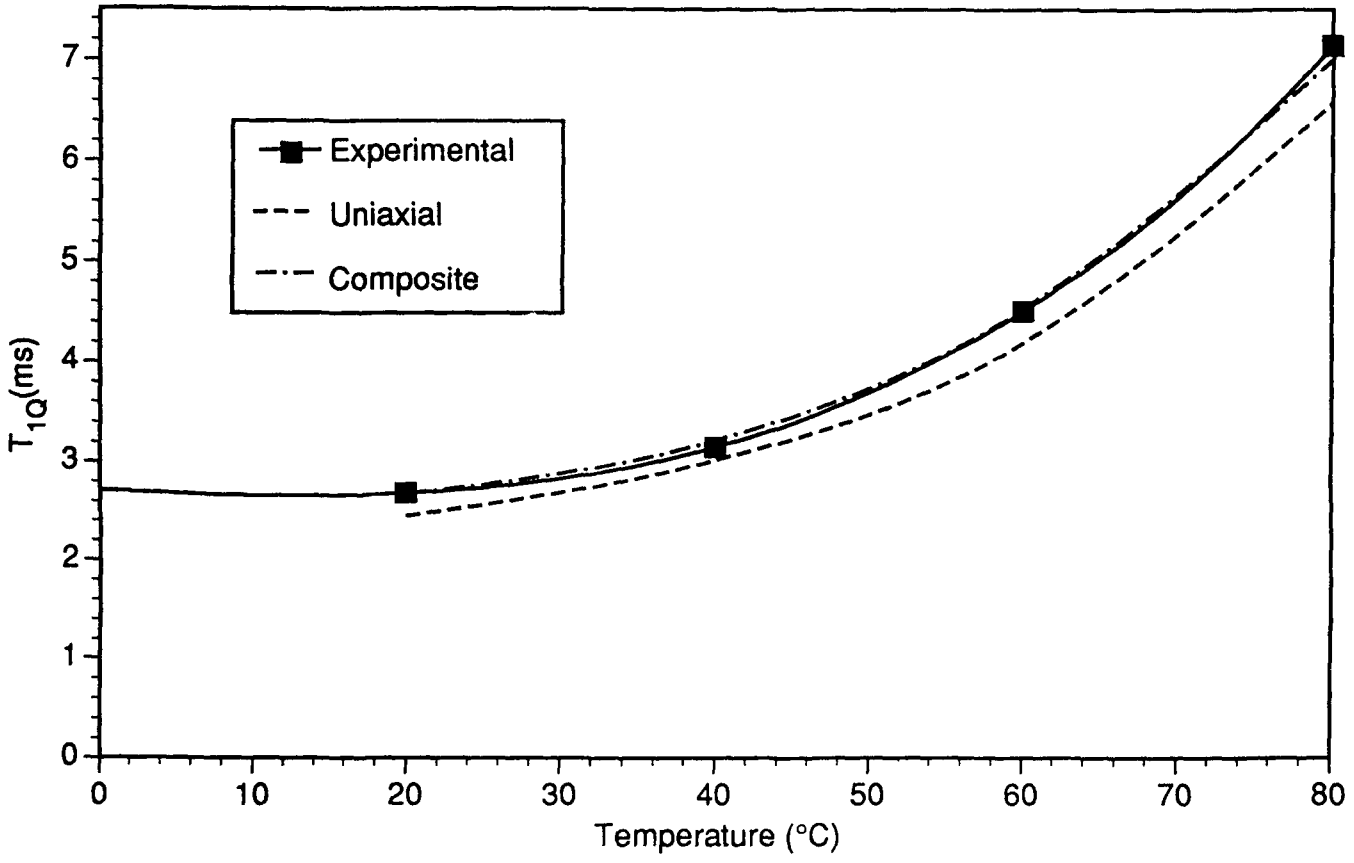

Figure 5. Broadband Jeener-Broekaert relaxation time constants for microcrystallites oriented at 15 degrees with respect to the magnetic field for deuterons on the phenyl ring of SHBS in the liquid crystalline phase with temperature.

Figure 6. Predicted rate constants for phenyl ring reorientation about the 1'-4' axis for the uniaxial(●) and composite (▲) models as a function of temperature.